Human Molecular Genetics, 2015, Vol. 24, No. 20 5867–5879

doi: 10.1093/hmg/ddv308
Advance Access Publication Date: 28 July 2015
Original Article

ORIGINAL ARTICLE

Loss of fibulin-4 disrupts collagen synthesis and maturation: implications for pathology resulting from *EFEMP2* mutations

Christina L. Papke[1], Jun Tsunezumi[1], Léa-Jeanne Ringuette[2], Hideaki Nagaoka[3], Masahiko Terajima[3], Yoshito Yamashiro[1,4], Greg Urquhart[1], Mitsuo Yamauchi[3], Elaine C. Davis[2] and Hiromi Yanagisawa[1,4,*]

[1]Department of Molecular Biology, The University of Texas Southwestern Medical Center, Dallas, TX 75390, USA, [2]Department of Anatomy and Cell Biology, McGill University, Montreal, Quebec H3A 0C7, Canada, [3]NC Oral Health Institute, University of North Carolina, Chapel Hill, NC 27599, USA and [4]Life Science Center, Tsukuba Advanced Research Alliance, University of Tsukuba, 1-1-1 Tennodai, Tsukuba, Ibaraki 305-8577, Japan

*To whom correspondence should be addressed. Tel: +1 2146487723; Fax: +1 2146481488; Email: hiromi.yanagisawa@utsouthwestern.edu

Abstract

Homozygous recessive mutations in either *EFEMP2* (encoding fibulin-4) or *FBLN5* (encoding fibulin-5), critical genes for elastogenesis, lead to autosomal recessive cutis laxa types 1B and 1A, respectively. Previously, fibulin-4 was shown to bind lysyl oxidase (LOX), an elastin/collagen cross-linking enzyme, *in vitro*. Consistently, reported defects in humans with *EFEMP2* mutations are more severe and broad in range than those due to *FBLN5* mutations and encompass both elastin-rich and collagen-rich tissues. However, the underlying disease mechanism in *EFEMP2* mutations has not been fully addressed. Here, we show that fibulin-4 is important for the integrity of aortic collagen in addition to elastin. Smooth muscle-specific *Efemp2* loss in mouse (termed SMKO) resulted in altered fibrillar collagen localization with larger, poorly organized fibrils. LOX activity was decreased in *Efemp2*-null cells, and collagen cross-linking was diminished in SMKO aortas; however, elastin cross-linking was unaffected and the level of mature LOX was maintained to that of wild-type aortas. Proteomic screening identified multiple proteins involved in procollagen processing and maturation as potential fibulin-4-binding partners. We showed that fibulin-4 binds procollagen C-endopeptidase enhancer 1 (Pcolce), which enhances proteolytic cleavage of the procollagen C-terminal propeptide during procollagen processing. Interestingly, however, procollagen cleavage was not affected by the presence or absence of fibulin-4 *in vitro*. Thus, our data indicate that fibulin-4 serves as a potential scaffolding protein during collagen maturation in the extracellular space. Analysis of collagen in other tissues affected by fibulin-4 loss should further increase our understanding of underlying pathologic mechanisms in patients with *EFEMP2* mutations.

Introduction

Mutations in EGF-containing fibulin-like extracellular matrix (ECM) protein 2 (*EFEMP2*), also known as fibulin-4, lead to autosomal recessive cutis laxa type 1B (ARCL1B; OMIM no. 614437). ARCL1B is characterized by a severe and diverse array of defects including aortic aneurysms and arterial tortuosity,

Received: April 17, 2015. **Revised:** June 24, 2015. **Accepted:** July 24, 2015

vessel stenosis, cutis laxa, skeletal and craniofacial anomalies, joint laxity, respiratory problems including diaphragm abnormalities and bradycardia (1–4). Fibulin-4 plays a critical role in elastogenesis *in vitro* (5–7), and conventional knockout of fibulin-4 in mice leads to severe disruption of elastic fiber assembly and perinatal lethality due to large ascending aortic aneurysms (8). Although both smooth muscle-specific fibulin-4 knockout mice and haploinsufficient mice are viable, these mice also develop ascending aortic aneurysms and vessel tortuosity (9,10). Interestingly, some of the observed phenotypes due to loss of fibulin-4 in humans, including bone fragility and other skeletal abnormalities, documented in multiple reports (1,2,4,11,12), may not be explained by the loss of elastic fibers alone, raising the question as to whether fibulin-4 has additional, extra-elastogenic functions (4).

The striking phenotypic differences in patients with *EFEMP2* mutations compared with mutations in *FBLN5*, encoding fibulin-5, further support the idea of extra-elastogenic roles for fibulin-4. Both fibulin-4 and fibulin-5 play critical, non-redundant roles in elastogenesis (6,13), and the phenotypes observed in patients with mutations in either gene are recapitulated in knockout mouse models (8,14,15). Although *FBLN5* mutations also lead to cutis laxa and disruption of elastic fibers, these mutations do not result in aortic aneurysm formation (OMIM no. 219100, ARCL1A). Thus, phenotypic comparison of *EFEMP2* and *FBLN5* mutations in patients, and in corresponding mouse models, strongly suggests that elastic fiber defects alone are insufficient to drive aneurysm formation. This notion is consistent with others who have hypothesized that fibulin-4 may have extra-elastogenic functions based on a broader array of proteins that bind fibulin-4 compared with fibulin-5 (16). Such extra-elastogenic roles for fibulin-4 and their implications for disease pathogenesis have not been investigated to date.

Several lines of evidence suggest that fibulin-4 may have a role in regulating collagen in addition to elastin. First, fibulin-4 interacts directly with pro-lysyl oxidase (LOX), an essential enzyme for elastin and collagen cross-linking (6,7). Second, *Efemp2*-null mice bear phenotypic similarities to *Lox*-null mice, and collagen abnormalities have been reported in the latter (17). These data suggest that fibulin-4 may be biologically relevant to collagen synthesis and maturation. Third, fibulin-4 deficiency results in increased trichrome staining for collagen in both mice and humans (1,9), indicating altered collagen synthesis. Finally, decreased collagen bundle size was observed in the dermis of a patient with a homozygous recessive mutation in *EFEMP2*, suggesting defective collagen fibrillogenesis (4). However, neither the biosynthesis of collagen, nor the maturation of collagen has been investigated in these mouse models.

Collagen synthesis, secretion, processing and assembly into fibrils is a complex, multi-step process (reviewed in 18–20). Briefly, collagen undergoes a number of post-translational modifications in the endoplasmic reticulum, including hydroxylation of lysine and proline residues, and is folded via the help of collagen-specific chaperones including SERPINH1, FKBP65 and foldases (21,22). Once secreted, the N- and C-terminal propeptides are cleaved by specific enzymes [ADAMTS proteases and tolloid metalloproteases including bone morphogenic protein 1 (BMP1), respectively], and mature collagen molecules self-assemble to form a fibril (18). After extensive post-translational modifications, additional molecules including small leucine-rich proteoglycans (SLRPs) regulate fibril growth (18). LOX catalyzes the reaction of oxidative deamination on the telopeptidyl lysine and hydroxylysine residues of collagen to initiate covalent intermolecular cross-linking. Disruption of any of these steps of collagen biosynthesis and maturation has been shown to affect the quantity and quality of collagen matrix.

Multiple studies have demonstrated the importance of collagen in maintaining vascular wall integrity. For instance, a decrease in type I collagen due to a deletion in first intron of the *Col1a1* gene leads to aortic dissection and rupture in mice in the absence of aortic dilatation (23–25). Also, mice haploinsufficient for *Col3a1* due to a spontaneous 185 kb deletion in the gene die from aortic rupture at 4–10 weeks with a median age of 6 weeks (26). These studies and others highlight the critical involvement of fibrillar collagen in aortic disease, particularly aortic dissection and rupture. Here, we show that the loss of fibulin-4 in smooth muscle cells (SMCs) leads to previously uncharacterized molecular defects in collagen biosynthesis. Since aortic aneurysms represent the most severe phenotypic feature of *EFEMP2* mutations, we chose to specifically analyze collagen biosynthesis and maturation in the aortic wall.

Results

Fibulin-4 loss alters fibrillar collagen protein expression and localization but not gene expression

Since type I, III and IV collagens represent the most abundant collagen subtypes in the aortic wall, we performed gene expression analysis and immunofluorescent staining of P90 aortas of wild-type (WT; $Efemp2^{+/+;SM22\text{-}Cre}$) mice and mice specifically lacking fibulin-4 in vascular SMCs ($Efemp2^{loxP/KO;SM22\text{-}Cre}$; termed SMKO; Ref. 9). QPCR did not show any difference in *Col1a1*, *Col3a1* or *Col4a1* gene expression (Fig. 1A). Immunofluorescent staining, however, revealed alterations in fibrillar collagen localization. The majority of type I and III fibrillar collagens were found in the adventitial layer in WT aortas, but in aortas of SMKO mice both of these collagens appeared less prominently in the adventitial layer but were increased in the medial layer (Fig. 1B). This was consistent with previous data showing an increase in type I collagen levels in SMKO aortas by western analysis (27). Type IV collagen showed variable expression levels in SMKO aortas but was consistently found in the basement membrane surrounding the SMCs in both control ($n = 7$) and SMKO ($n = 11$) aortas. Overall, the protein was more disorganized in SMKO aortas, likely due to the SMC disarray in these aortas (data not shown) (9). Since type V collagen acts as an initiator of fibril assembly (28) and regulates the number and size of collagen fibrils present (29,30), we also examined type V collagen expression in the aortic wall, but did not find any difference in localization or expression levels by immunofluorescence in SMKO aortas compared with WT (Supplementary Material, Fig. S1A).

We sought to determine differences in organization and structure of fibrillar collagens in SMKO aortas. Second harmonic generation (SHG) imaging provides a method for specific imaging of fibrillar collagen (mainly type I collagen) without the use of antibodies and provides higher resolution imaging than is available with antibody labeling (31). Furthermore, SHG and two-photon-excited fluorescence (TPEF) have been shown to be highly effective for simultaneously analyzing collagen and elastin, respectively, in the aortic wall (32,33). In WT aortas, SHG signal (green) was strongest in the adventitia, but in SMKO aortas, strong SHG signal extended past the adventitia well into the medial layer containing fragmented elastic fibers (TPEF signal, red), similar to the collagen localization pattern observed by immunofluorescence (Fig. 1C). Collagen bundles in ascending aortas of P90 mice appeared disorganized in SMKO, in contrast to those seen in WT mice, particularly in the adventitia, which were aligned in a wave-like pattern. Additionally, the increased punctate appearance of the collagen was suggestive of decreased

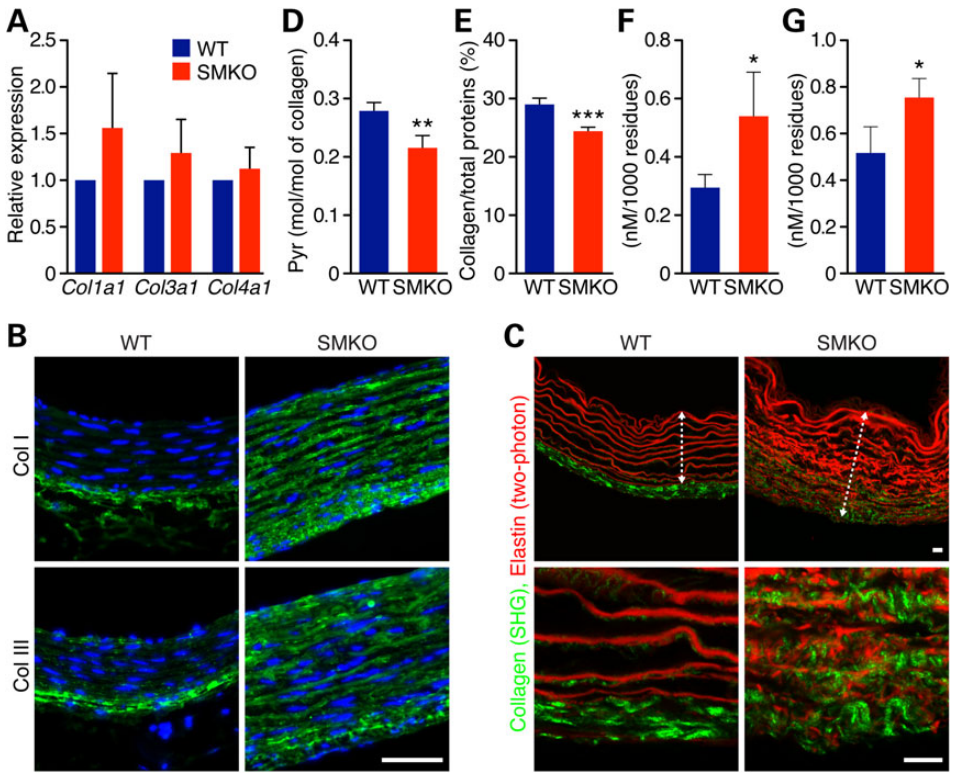

Figure 1. Loss of fibulin-4 leads to alterations in collagen localization, organization and cross-linking but not gene expression. (**A**) Quantitative PCR of *Col1a1*, *Col3a1* and *Col4a1* showed no difference in gene expression in smooth muscle-specific knockout (*Efemp2*$^{loxP/KO;SM22\text{-}Cre}$; termed SMKO) versus wild-type (*Efemp2*$^{+/+;SM22\text{-}Cre}$; termed WT) aortas ($n = 3$). (**B**) Collagen type I (Col I) and type III (Col III) are increased in the medial layer of SMKO ascending aortas, whereas the majority of these proteins are found in the adventitia of WT mice. Scale bar represents 50 µm. WT, $n = 3$; SMKO, $n = 4$ aortas. Samples are oriented with the vessel lumen at the top and adventitia on the bottom. (**C**) SHG (green) imaging of collagen fibers and two-photon imaging of elastic fibers (TPEF; red) confirm an increase of fibrillar collagen in the medial layer of SMKO aortas and indicate a disorganization of collagen fibers in SMKO. Scale bars represent 50 µm. White dotted lines in lower panels denote medial layer. $N = 3$ aortas per genotype. (**D**) HPLC analysis of mature collagen cross-links showed a 23% decrease in cross-linking in SMKO compared with WT. (**E**) HPLC analysis of collagen content (normalized to amounts of total protein present in each sample) showed a significant decrease in collagen in SMKO aortas (**F** and **G**). Desmosine (F) and isodesmosine (G) were increased in SMKO aortas compared with WT using a Student's *t*-test. In (D–G), $n = 4$ for each genotype; $^*P < 0.05$, $^{**}P < 0.01$, $^{***}P < 0.001$.

collagen maturity. Thus, loss of fibulin-4 leads to disorganization and redistribution of fibrillar collagen in the aortic wall.

Fibulin-4 loss decreases collagen content and maturation

The final step in collagen maturation is cross-linking, a multi-step process initiated by the lysyl oxidase family of enzymes. Since others have shown that fibulin-4 directly interacts with LOX, and our SHG data were suggestive of immature and/or disorganized collagen fibers, we hypothesized that fibulin-4 loss might lead to a decrease in LOX-mediated collagen cross-linking. We performed HPLC analysis on P90 aortas and found a 23% decrease in mature collagen cross-linking, pyridinoline (Pyr) in SMKO compared with WT, which was statistically significant (Fig. 1D). Deoxypyridinoline was not quantified due to the limited quantity in these samples. Surprisingly, however, despite the appearance of more collagen in the aortic wall via immunofluorescence, we found a 16% decrease in collagen content measured as hydroxyproline/total protein in SMKO aortas compared with WT ($P < 0.001$) when normalized to total amounts of protein (Fig. 1E). We also previously showed aortic wall thickening in SMKO mice, and thus it is possible that the increase in other vessel wall components results in a net decrease in collagen content in our calculations (9). Thus, in the SMKO aortic wall, not only is relative collagen content lower, but the content of mature cross-link per collagen is also diminished in comparison with WT.

Since LOX also catalyzes the cross-linking of elastin, we analyzed two of the elastin-specific cross-links, desmosine and isodesmosine, in aortas. In contrast to collagen cross-links, we found a significant increase in both desmosine and isodesmosine in SMKO, indicating that the loss of fibulin-4 selectively leads to decreased collagen but not elastin cross-linking, despite clear disruption of elastic fiber structure (Fig. 1F and G). This is in sharp contrast to a *Lox*-null mouse model, in which desmosine content was decreased by ~60% (34).

Aortic collagen fibril diameter is increased and fibril organization is highly disrupted

The decrease in mature collagen, along with the appearance of abnormal collagen structure via SHG imaging, led us to examine the structural defects in collagen in greater detail. Electron microscopy (EM) of the thoracic aorta showed highly irregular collagen fibrils in the SMKO compared with WT at P90, a time point when aneurysms are fully established (Fig. 2A and B). Collagen fibril size was highly variable in SMKO aortas, with numerous large fibrils as well as some that were abnormally small in size. Additionally, fibrils in SMKO aortas exhibited profound disorganization and appeared more loosely packed than those in WT aortas. Quantification of fibril diameter confirmed a wider distribution of fibril diameters in SMKO compared with WT aortas, along with an overall increase in fibril size, which was statistically significant (48.89 ± 10.03 nm

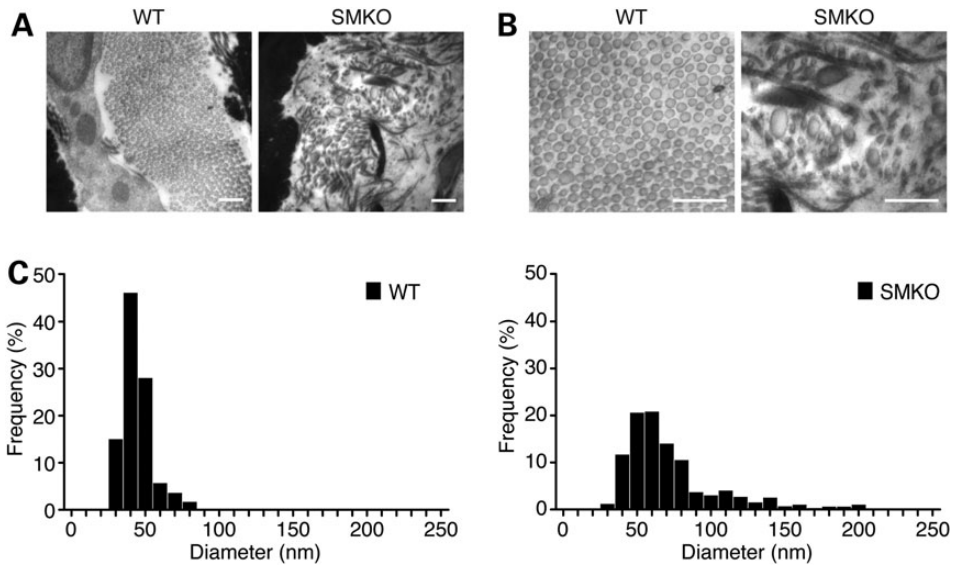

Figure 2. Fibulin-4 loss leads to disorganized collagen fibrils with irregular shape and increased size (**A** and **B**). EM images showing collagen fibrils in P90 WT and SMKO aortas. Note highly irregular and disorganized collagen fibrils in SMKO. Higher magnification images are shown in (**B**). Scale bars represent 500 nm. (**C**) Quantification of fibril diameter showed a wider distribution of fibril size in SMKO aortas, consistent with visual observations. Mean diameter of fibrils was significantly increased in SMKO. One thousand fibrils from each genotype (500 fibrils each from $n = 2$ aortas) were measured.

in WT versus 77.73 ± 34.75 nm in SMKO; $P < 0.0001$; Fig. 2C). In addition to highly variable (but overall larger) fibril diameters, disorganization of fibrils and decreased bundle density were observed in SMKO compared with smooth and homogenous fibrils seen in WT, suggesting that one or more molecules involved in controlling fibril shape and/or size may also be affected by fibulin-4 loss. Interestingly, fibulin-5 deficiency, which also leads to elastic fiber defects, does not induce disruption in collagen fibrils (unpublished observations), suggesting that loss of elastic fiber integrity alone may be insufficient to drive the observed collagen defects. Based on the appearance of loosely packed collagen fibrils, we examined other non-collagenous ECM components to determine whether an increase in any of these components may contribute to the altered fibril density. Increased proteoglycan accumulation is a hallmark feature of aortic aneurysms, and Alcian blue staining showed an increase in glycosaminoglycan associated with proteoglycans in SMKO aortas compared with WT (Supplementary Material, Fig. S1B). It is possible that proteoglycan accumulation contributes to the decreased fibril density. Fibronectin 1 forms a critical scaffold for other ECM proteins, including fibrillar collagen and fibrillin (35,36); therefore, we also examined fibronectin 1 expression and localization, but found no difference between WT and SMKO aortas (Supplementary Material, Fig. S1C).

LOX gene expression but not LOX processing is altered *in vivo*, and LOX activity is decreased in matrix and conditioned media *in vitro*

We next sought to determine the mechanism(s) driving the observed collagen defects in SMKO aortas. Since fibulin-4 is known to interact directly with LOX and many phenotypic similarities exist between conventional *Efemp2*-null and *Lox*-null mice (8,34,37), we analyzed LOX expression, localization, processing and activity *in vitro* and *in vivo*. LOX activity in conditioned media from *Efemp2* germline knockout ($Efemp2^{-/-}$; termed GKO) mouse embryonic fibroblasts (MEFs) was decreased by 35.49 ± 10.72% compared with $Efemp2^{+/+}$ littermate controls (WT), which was statistically significant ($P < 0.05$; Fig. 3A). Analysis of ECM extracts from both WT and GKO samples yielded similar results, with a slight decrease in LOX activity per micrograms of total protein in GKO extracts compared with WT, although this did not reach statistical significance (Fig. 3B).

Full-length pro-LOX is inactive but is activated by proteolytic cleavage of the propeptide region; therefore, detecting LOX propeptide can provide an indirect estimate of the amount of cleaved (active) LOX present in tissue samples. Immunofluorescent labeling with an antibody directed against the propeptide region of LOX (LOX-pp) showed similar localization of LOX-pp throughout the aortic wall in both control (Ctl; $Efemp2^{+/+;SM22\text{-}Cre}$ or $Efemp2^{KO/+;SM22\text{-}Cre}$) and SMKO P30 aortas, with increased expression in SMKO (Fig. 3C). Since immunofluorescence only showed the total amount of LOX-pp (both cleaved from LOX and uncleaved), we performed immunoblotting on aortic tissue extracts and found a significant increase in total LOX (cleaved + uncleaved) in SMKO aortas (Fig. 3D). The amount of full-length LOX was also significantly increased in SMKO. We did observe a slight decrease in the calculated percentage of cleaved LOX-pp versus uncleaved LOX, but this did not reach statistical significance, and the fact that both full-length LOX and LOX-pp were increased in SMKO aortas suggests that greater amounts of active LOX should be available within the aorta of SMKO and that the decreased collagen cross-linking is not due to a simple loss of LOX activity (Fig. 3E).

It is surprising that despite the striking disorganization of collagen in the SMKO aortas, along with many phenotypic similarities between the *Lox*-null mice and *Efemp2*-null mice, the observed decrease in LOX activity does not appear to match the amount of decrease in LOX activity in the *Lox*-null mice (17). These data therefore imply that while a decrease in LOX activity may be partially responsible for the collagen defects in SMKO mice, additional mechanisms also play an important role in collagen synthesis and maturation in SMKO aortas. It is also interesting to note that despite decreased LOX activity in GKO conditioned media and ECM extracts, we did not observe increased LOX expression by immunofluorescence or immunoblotting and did not detect a difference in LOX cleavage (Supplementary Material, Fig. S2).

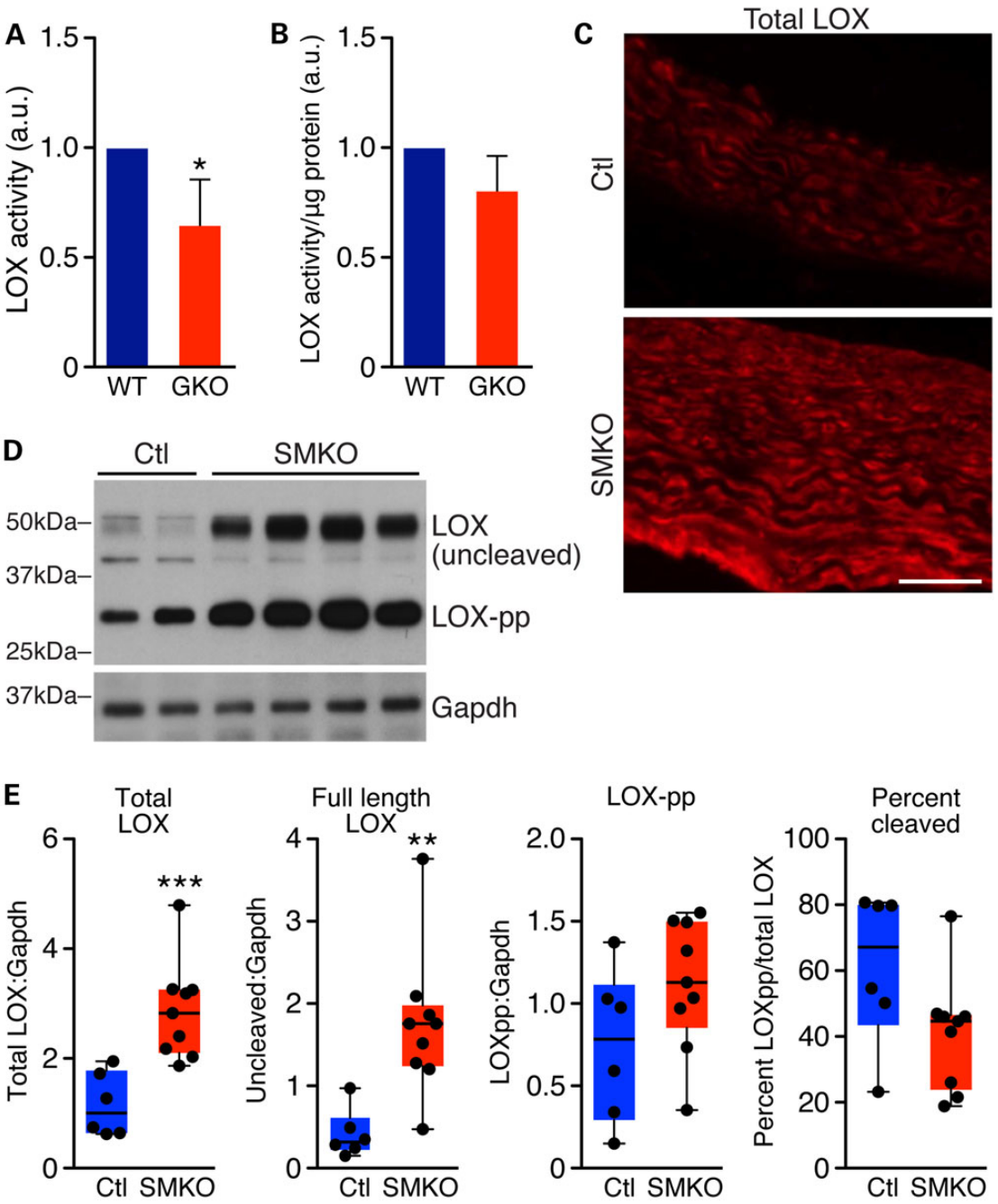

Figure 3. LOX activity is decreased *in vitro* but LOX cleavage is normal *in vivo*. (**A**) LOX activity was significantly decreased in conditioned media from GKO MEFs, $^{*}P < 0.05$. (**B**) LOX activity was also slightly decreased in ECM extracts from GKO MEFs (not significant). Values were obtained by subtracting the amount of fluorescent signal inhibited by the LOX inhibitor βAPN from the total amount of fluorescent signal for each sample. (**C**) Immunofluorescent staining using a LOX-pp antibody that recognizes both cleaved and uncleaved LOX showed increased staining intensity in P30 SMKO aortas. Scale bar represents 50 µm. (**D**) Immunoblot showing both uncleaved LOX and LOX propeptides are increased in SMKO aortas. Representative immunoblot data are shown; $n = 6$ WT and $n = 9$ SMKO aortas were used for quantification and analysis. (**E**) Quantification of immunoblot in (D). Total LOX and full-length (uncleaved) LOX were significantly increased in SMKO aortas. LOX propeptide (LOX-pp) was increased and the calculated percentage of cleaved LOX was slightly decreased in SMKO aortas, but were not statistically significant. Error bars represent ±SD. $^{**}P < 0.01$, $^{***}P < 0.001$.

Multiple proteins involved in the collagen maturation process are putative fibulin-4-interacting proteins

To identify binding partners of fibulin-4 that are potentially involved in collagen maturation, we used affinity purification and mass spectrometry. Rat vascular SMCs were infected with adenovirus containing either fibulin-4 with a C-terminal V5 tag (Ad5-fib4-V5) or control adenovirus containing GFP (Ad5-GFP) with MOI 200. Two days after infection, the cells were incubated for 18 h in 2% fetal bovine serum (FBS), and conditioned media and cell lysates were harvested. Since immunoprecipitation may fail to detect weaker and/or more transient protein–protein interactions, proteins were reversibly cross-linked to preserve

Table 1. Potential fibulin-4-interacting proteins identified by mass spectrometry

Proteins identified by mass spectrometry	Peptides identified	Percent coverage	Function in collagen regulation	References
Collagen α1(I), α2(I)	30, 41	35.3, 43.2	Highly abundant collagen in aortic wall	(65)
Serpin H1 (Hsp47)	16	41.2	Collagen protein folding in ER	(66)
Procollagen C-endopeptidase enhancer 1	7	20.3	Enhances BMP1-mediated C-propeptide cleavage	(67)
Fibromodulin	8	27.9	Fibril size/organization	(44)
Biglycan	3	7.6	Fibril size/organization	(57)
Lactadherin	10	22.2	Collagen removal from tissue	(68)
Lysyl oxidase	9	35.5	Collagen cross-linking	(69)

these interactions (38). Concentrated media and cell lysate were immunoprecipitated with V5 antibody and run a short distance onto a polyacrylamide gel. Entire bands were excised and subjected to mass spectrometric analysis. We obtained a number of potential interacting proteins that are known to be directly involved in regulating collagen synthesis, maturation and assembly, including Pcolce, Col1a1, Col2a1 and fibromodulin, an SLRP (Table 1). Several proteins known to interact directly with fibulin-4, including elastin and LOX, were also identified by the screen, confirming the validity of the results (Supplementary Material, Tables S1 and S2).

Fibulin-4 directly interacts with Pcolce but does not affect Pcolce activity *in vitro*

Cleavage of N- and C-terminal propeptides is an important regulatory step in collagen processing and assembly into fibrils, and problems with either of these steps lead to defects in fibril formation. Cleavage of the C-terminal propeptide is mediated by BMP1, and this reaction is enhanced by Pcolce. Since Pcolce was identified by our proteomic screen as a potential fibulin-4 binding partner, we performed solid-phase binding assays using commercially available Pcolce (R&D Systems, Inc.) and purified fibulin-4 containing a C-terminal V5-His tag (fibulin-4-V5) as a soluble ligand (Supplementary Material, Fig. S3A and B). Soluble fibulin-4 showed moderate binding to Pcolce in a dose-dependent manner (Fig. 4A). Tropoelastin was used as a positive control and showed a similar binding pattern to fibulin-4 as Pcolce (Fig. 4B).

Based on the observed interaction, we hypothesized that fibulin-4 might act as an enhancer of Pcolce activity and that its loss might therefore lead to a disruption of C-terminal propeptide cleavage. BMP1 and Pcolce were incubated in the presence or absence of fibulin-4 for 45 min at 37°C, with short forms of either collagen I or III containing intact N- and C-terminal domains (R&D Systems) as a substrate. Uncleaved short collagen type I was slightly decreased and C-propeptide was increased by incubation with BMP1. Based on silver staining, in the presence of Pcolce, uncleaved collagen type I was significantly decreased and cleaved C-propetide was increased: however, the cleavage was not further enhanced by the presence of fibulin-4 (Fig. 4C and D; compare lanes 3 and 5 in Fig. 4C). It has been shown that heparin potentiates BMP1 and Pcolce-mediated cleavage of short type I collagen *in vitro* (39), and both Pcolce and fibulin-4 have been shown to bind heparin (40,41). However, fibulin-4 did not exhibit any effects on the cleavage of short type I collagen in either the presence or absence of heparin (Fig. 4C and D). Similar results were obtained using short type III collagen as a substrate (Supplementary Material, Fig. S3C and D). We also

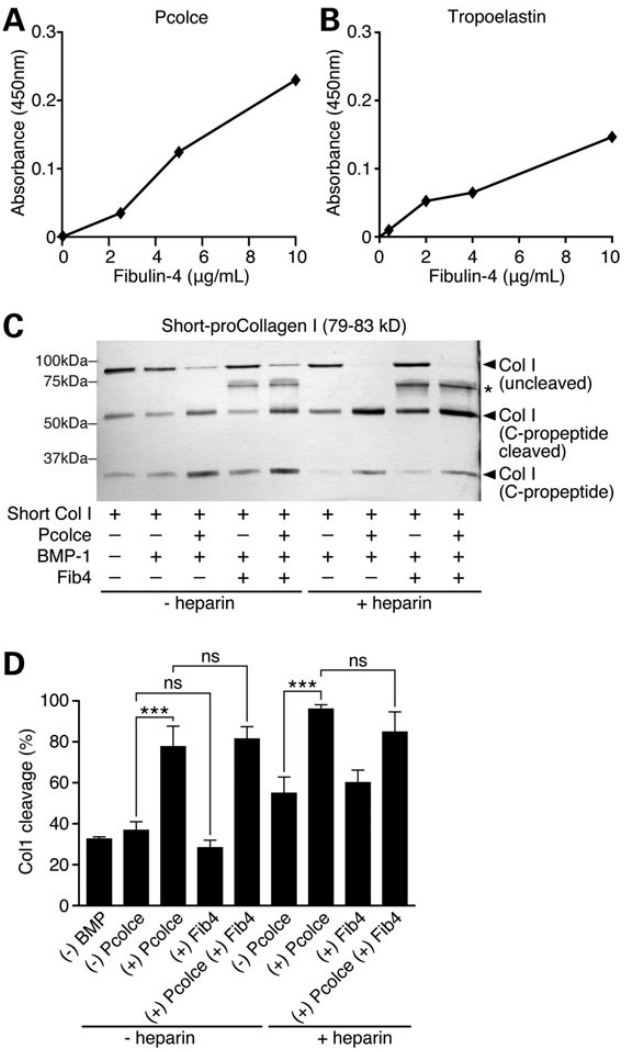

Figure 4. Fibulin-4 interacts with Pcolce but does not affect its activity *in vitro*. (**A** and **B**) Fibulin-4 binds to Pcolce (A) and tropoelastin (B). Representative solid-phase binding assay using Pcolce or tropoelastin as the solid-phase and increasing concentrations of fibulin-4 as soluble ligand. Bovine serum albumin (BSA) was used as a negative control, and data are shown with values for BSA binding subtracted from the final values. $N > 3$ independent experiments. (**C** and **D**) Pcolce enhances BMP1-mediated cleavage of a short form of the α1 chain of type I collagen, but adding fibulin-4 does not further enhance the cleavage, either in the presence or absence of heparin. Representative silver stain is shown in (C), and quantification of $n = 3$ independent experiments is shown in (D). Error bars represent ±SEM. Similar results were observed using a short form of Col3a1 (Supplementary Material, Fig. S3C and D). Asterisk denotes fibulin-4.

performed immunofluorescent staining and observed Pcolce expression in both WT and SMKO aortas, although Pcolce staining appeared stronger toward the outer medial layer and adventitial layer of SMKO aortas (Supplementary Material, Fig. S4). Thus, fibulin-4 binds Pcolce but may play more of a role in localization of Pcolce rather than directly affecting Pcolce/BMP1-mediated C-terminal collagen propeptide cleavage *in vitro*.

Discussion

Our results show that fibulin-4 is important for the integrity of collagen in the aortic wall, in addition to its already well-established role in elastic fiber formation. Specifically, we found that the loss of fibulin-4 in vascular SMCs leads to accumulation of collagen fibers in the aortic media that are highly disorganized and irregular in shape and size. In contrast, deletion of fibulin-5, which also disrupts elastic fibers in the aortic wall, does not affect collagen, suggesting that fibulin-4 plays a non-redundant role in maintaining collagen integrity in the vessel wall. Furthermore, alterations in fibril size and shape have been observed in other mouse models and in human disease, including decorin-, lumican- and fibromodulin-deficient mouse models (42–44), classical Ehlers-Danlos Syndrome Type I and II (45), Ehlers-Danlos Syndrome type VIIA and VIIB (46) and Osteogenesis Imperfecta (47,48), providing evidence that the structural changes observed in SMKO mice are likely to be biologically relevant.

Among 29 collagen types, there are 7 fibrillar collagens (I–III, V, XI, XXIV and XXVII), with types I and III being the most abundant collagens in the aorta (49). Collagen fibrils are organized into fiber bundles arranged in a parallel manner in normal aortas (50) and provide tensile strength to the vessel wall (51). Although fibulin-4 has been shown to interact with type IV collagen, we did not observe differences in type IV collagen localization and failed to find differences in expression levels between WT and SMKO aortas. Surprisingly, there was no observed increase in *Col1a1* or *Col3a1* gene expression, despite our previous observations of increased angiotensin II and TGFβ1-dependent signaling, which are known stimulators of collagen production in SMCs (52,53). It is possible that other regulatory mechanisms control or limit the accumulation of these mRNAs.

Contrary to our expectations and despite phenotypic similarities between *Efemp2*-null and *Lox*-null mice, our data suggest that the observed type I collagen defects are not solely attributable to a loss of LOX activity. We found an overall 16% decrease in total collagen content in SMKO mice, compared with a ~25% decrease in *Lox*-null aortas, as measured by hydroxyproline content (34). Furthermore, we found a 23% decrease in mature collagen cross-link, pyridinoline, when normalized to collagen. This implies that not only is overall collagen content decreased, but cross-linking 'in' collagen is also defective. Thus, the net effect of these decreases on mechanical properties of the aorta could be significant. We further found a decrease in LOX activity in both MEFs and ECM extracts from MEF cells in culture, although the latter failed to reach statistical significance. In contrast, *Lox*-null mice displayed a large decrease in immature collagen cross-links [43% reduction in DHLNL (dihydroxylysinonorleucine), and 39% reduction in HLNL (hydroxylysinonorleucine)] and an ~80% decrease in LOX activity in cultured SMCs (17,34). Additionally, we found that LOX expression was increased *in vivo*, and LOX was cleaved nearly as efficiently in SMKO aortas as in WT with a small decrease that did not reach statistical significance. It has previously been shown that fibulin-4 binds LOX-pp and suggested that fibulin-4 plays a role in LOX localization for proper function in elastin cross-linking (7). Interestingly,

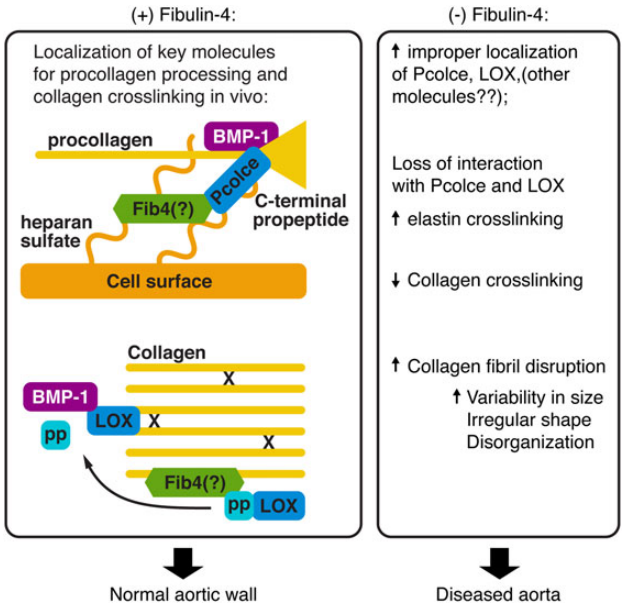

Figure 5. Model: Fibulin-4 as a scaffolding protein for proper localization of Pcolce in addition to LOX. We propose a role for fibulin-4 in stabilization of Pcolce/procollagen complex for BMP1 cleavage of collagen C-terminal propeptide, similar to a previously published proposal for heparin interaction with Pcolce, collagen, heparan sulfate proteoglycans and BMP1 (39). In the absence of fibulin-4, this localization is likely disrupted.

cross-linking of elastin was not decreased in SMKO aortas but was even paradoxically increased. This is in sharp contrast to *Lox*-null mice, in which desmosine content was reduced by ~60% (34). Although collagen fibrils appear disorganized in other tissues via EM analysis in *Lox*-null mice, one study reported no difference in collagen fibril diameters in the *Lox*-null aortas, in direct contrast to the significant increase in fibril size and broader distribution of fibril diameters observed in SMKO aortas (34). Thus, collagen was severely disorganized in SMKO aortas, but cross-linking and loss of LOX activity were not as severe as in *Lox*-null mice. These differences suggest that additional mechanisms may control fibril size and organization in SMKO aortas.

Further investigation of the mechanism(s) driving the collagen defects led us to examine Pcolce identified through our Co-IP and proteomic screening. Solid-phase binding assays confirmed binding between fibulin-4 and Pcolce, although binding was less strong than reports showing fibulin-4 binding to elastin or LOX. Surprisingly, however, fibulin-4 did not affect the ability of Pcolce to enhance BMP1-mediated cleavage of the procollagen C-terminal propeptide in either the presence or the absence of heparin in cleavage assays. Together with the finding that total loss of Pcolce in mice leads to collagen fibril abnormalities in multiple tissues including bone and tendon (54), our data suggest that the role of fibulin-4 in collagen fibril maturation is not directly potentiating the function of Pcolce, but rather serving as an important scaffolding protein to bring Pcolce and LOX in close proximity to ensure efficient collagen cross-linking during fibrillogenesis (Fig. 5). Accordingly, the function of fibulin-4 may be more critical in conditions in which collagen turnover and/or remodeling increases such as hypertension or aneurysm expansion (55,56). Since BMP1 cleaves LOX in addition to fibrillar collagen, it is also possible that the absence of fibulin-4 may liberate more Pcolce and enhance BMP1-mediated collagen cleavage but decrease BMP1-mediated LOX maturation, resulting in inefficient collagen fibril formation.

In future studies, it would be interesting to determine whether fibulin-4 plays a role in correct localization of other proteins. Additionally, it will be fascinating to observe whether interaction of fibulin-4 and Pcolce (and potentially other proteins involved in collagen regulation) plays an important role in other tissues such as tendons and ligaments, where collagen content is much higher than in the vessel wall. Results from our proteomic screen suggest that fibulin-4 may interact with one or more of the SLRPs, which could in turn contribute to the observed collagen defects. Mice lacking biglycan, an SLRP, develop irregular collagen fibrils similar to what we observed in SMKO mice, and aortas spontaneously rupture in males when mice are ~3 months old (57). Loss of other SLRPs, including fibromodulin, decorin and lumican, or a combination of these proteins, also lead to disruptions in collagen fibrillogenesis (42–44). Fibromodulin was recently shown to inhibit LOX-mediated cross-linking on the C-telopeptide of collagen, suggesting a mechanism by which fibromodulin may help prevent premature fibril assembly and constrain fibril growth (58). It will be interesting to see in future studies whether fibulin-4 interacts with these SLRPs.

In summary, we have expanded the interaction network of fibulin-4 to include Pcolce and characterized a previously unstudied role for fibulin-4 in regulating collagen maturation in the vascular wall. Given the wide array of abnormalities in both collagen- and elastin-rich tissues observed in patients with *EFEMP2* mutations, our study suggests that a more detailed analysis of collagen in other tissues affected by the loss of fibulin-4 would prove useful, both for gaining a better understanding of the underlying pathologic mechanisms and for developing more effective ways to treat these and other connective tissue disorders.

Materials and Methods

Mice

All mouse studies were approved by the University of Texas Southwestern (UTSW) Medical Center Institutional Animal Care and Use Committee. Animals were housed in the UTSW Animal Resource Center, and all procedures were carried out in accordance with NIH Guidelines for the Care and Use of Laboratory Animals. Smooth muscle-specific and germline *Efemp2* knockout mice were generated as described previously (RRID:MGI_4947945; Tg(CAG-cre)13Miya;Efemp2$^{tm1.Hiya}$/Efemp2$^{tm1.Hiya}$ and Tg(Tagln-cre)1Her;Efemp2$^{tm1.1Hiya}$/Efemp2$^{tm1.2Hiya}$) (9). Mice wild type for Efemp2 but containing the Tagln-Cre (SM22-Cre) transgene (*Efemp2*$^{+/+;SM22\text{-}Cre}$) were used as WT for comparison with *Efemp2*$^{loxP/KO;SM22\text{-}Cre}$ (SMKO) mice. Mice heterozygous for Efemp2 containing the Tagln-Cre transgene (*Efemp2*$^{KO/+;SM22\text{-}Cre}$) showed no phenotypic differences as previously observed (59) and were also included for comparison where indicated as Ctl.

Quantitative PCR

Whole aortas were carefully dissected from P90 SMKO and control mice. Following tissue homogenization, mRNA was isolated using an RNeasy mini kit (Qiagen) and quantified on a Nanodrop. Equal amounts of mRNA were reverse transcribed using an iScript cDNA synthesis kit, and real-time PCR was performed using iTaq supermix containing SYBR green (Bio-Rad). QPCR primers used were as follows: *Col1a1* (CCAAGGGTAACAGCGGTGAA fwd; CCTCGTTTTCC TTCTTCTCCG rev), *Col3a1* (TCAAGTCTGGAGTGGGAGG fwd; TCCA GGATGTCCAGAAGAACCA rev), *Col4a1* (TACCATGGATACTCTCTGC TCTATGTC fwd; TGCCAGCCGTACCCAAGT rev), *Gapdh* (AGTATG ACTCCACTCACGGCAA fwd; TCTCGCTCCTGGAAGATGGT rev) and *B2M* (CCGAGCCCAAGACCGTCTA fwd; AACTGGATTTGTAAT TAAGCAGGTTCA rev). Data from at least three aortas per genotype were obtained and were normalized to *Gapdh* and β2 Microglobulin (*B2M*). Quantification was performed using the ΔΔCt method, and data were analyzed using a Student's *t*-test, with *P*-values of <0.05 considered statistically significant.

Immunofluorescence and second harmonic generation imaging

Phosphate-buffered saline (PBS)-perfused aortas were harvested from P30 and P90 mice and immediately embedded in OCT for cryosectioning. For two photon imaging, 20 µm transverse sections were mounted on glass slides and kept frozen. Immediately before imaging, samples were thawed to room temperature, hydrated with PBS and coverslipped. SHG and TPEF were used to visualize collagen and elastin, respectively, using a Zeiss LSM780 microscope (Carl Zeiss Microscopy, Thornwood, NY, USA) with a Chameleon Vision II Ti:Sapphire laser (Coherent, Inc.). SHG and TPEF were excited at 810 nm and imaged with a LD C-Apochromat ×40/1.1 W Korr objective lens. Backscattered SHG was separated from TPEF using a 380-430/470-520 filter set (Zeiss LSM BiG 1756-082) and detected with a non-descanned GaAsP detector.

For lysyl oxidase, type V collagen and Pcolce immunostaining, 10 µm cryosections were fixed for 10 min in 4% PFA, blocked 1 h in 5% normal goat serum and incubated with primary antibody [LOX-pp (1:100; kindly provided by P. Trackman) (60), type V collagen (1:100; Novus Bio no. NBP1-19633) or Pcolce (1:100; MyBioSource no. MBS2004251)] overnight. Sections were incubated with an AlexaFluor 568-conjugated secondary antibody (1:200; Invitrogen no. A-11011). Sections were mounted with Vectashield mounting medium with DAPI (Fisher, no. H-1200) and imaged using either an Axio Observer (Zeiss) for non-confocal imaging or either a Zeiss LSM500 or Nikon A1R microscope for obtaining confocal images. For collagen I, III and IV and fibronectin-1 immunostaining, P90 aortas were perfused with PBS followed by 4% PFA, fixed overnight at 4°C in 4% PFA and processed for paraffin embedding. Five-micrometer sections were mounted on slides, deparaffinized and rehydrated through a series of alcohols. Antigen retrieval was performed using sodium citrate buffer (pH = 6.0). Samples were blocked in 10% normal goat serum +0.3% Triton-X-100 for 1 h, followed by type I or III collagen (Abcam no. ab34710 and no. ab7778, respectively, 1:100), type IV collagen (Millipore Ab756P, 1:100) or fibronectin-1 (Abcam no. ab6328, 1:100) antibodies overnight at 4°C. The appropriate secondary antibody (AlexaFluor 488, 1:100; Invitrogen no. A11001 or no. A11008) was incubated for 1 h followed by DAPI (1:100; Sigma no. D9542) for 30 min, and sections were mounted with 50% glycerol/50% phosphate-buffered saline prior to imaging using an Axio Observer microscope. SHG/TPEF and confocal images were processed and analyzed using Zen software (Zeiss) or NIS Elements (Nikon). For non-confocal fluorescence microscopy, images were analyzed using Axiovision software (Zeiss).

Collagen and elastin cross-linking analysis and collagen quantification

Ascending aortas from P90 mice ($n = 6$ per genotype; three samples were pooled for one part of the analysis, and for the other part of the analysis, three samples were analyzed individually, for a final n of 4 independent runs) were pulverized in liquid nitrogen, washed with cold PBS then with distilled water and lyophilized. An aliquot of each (~1 mg) was hydrolyzed with 6N HCl and

subjected to amino acid and cross-link analyses as previously described (61). The collagen content was estimated as a percent of collagen in total protein based on the value of 100 residues of hydroxyproline per 1000 amino acids in collagen. The amounts of pyridinoline and deoxypyridinoline were expressed as moles/mole of collagen. Desmosine and isodesmosine content was also quantified as nanomolar concentrations per 1000 amino acids.

EM and quantification of collagen fibril size

P90 SMKO and WT mice were perfused with PBS to clear blood, followed by 3% glutaraldehyde in 0.1% sodium cacodylate (pH = 7.4) to fix the tissues. Following dissection, aortas were fixed further overnight. Aortas were treated sequentially with osmium tetroxide, tannic acid and uranyl acetate and dehydrated and embedded in Epon as previously described (62). Sixty-nanometer sections were counterstained with 7% methanolic uranyl acetate and lead citrate and observed using Tecnai 12 transmission electron microscope operating at 120 kV. All images were obtained at ×13 000 magnification and were analyzed using ImageJ software (NIH). Images were calibrated so that each image contained 500 pixels/nm. To reduce background noise and facilitate quantification of individual collagen fibrils, the threshold of each image was uniformly adjusted to mid-gray. For quantification of fibril size, 500 fibrils were randomly selected for quantification from each mouse, for a total of 1000 fibrils per genotype. Fibril diameter was calculated from the area using the following formula, $D = \sqrt{(A/\pi)}$. Statistical analyses were performed using GraphPad Prism software. A Student's *t*-test was used to determine statistical significance of fibril size, with *P*-values ≤ 0.05 considered significant.

Adenoviral transduction, immunoprecipitation and proteomic analysis

Adenoviruses containing either fibulin-4 with a C-terminal V5 tag (Ad5-fib4-V5) or GFP (Ad5-GFP) were generated and titrated. Primary rat aortic SMCs (Lonza no. R-ASM-580) were cultured in Dulbecco's modified Eagle's medium (DMEM) containing 20% FBS, 20 mM HEPES, 1 mM sodium pyruvate, antibiotic/antimycotic, 2 mM L-glutamine, ITS supplement (Sigma no. I3146–5 ml), 20 ng/ml basic fibroblast growth factor and 5 ng/ml epidermal growth factor. Cells at ~50–60% confluence were treated with either Ad5-fib4-V5 or Ad5-GFP at a range of MOIs (100–1000), and an optimal MOI was determined at 48 h post infection. MOI 200 was selected as the minimum dose required to obtain 95–100% GFP-positive cells. Rat SMCs were incubated with Ad5-fib4-V5 or Ad5-GFP for 16–18 h and washed with PBS, and fresh culture media were added. Two days after infection, the cells were incubated for 18 h in 2% FBS. Conditioned media were collected and concentrated using centrifugal concentrators (Millipore, 3000 MWCO). Cell layers were washed with PBS, and reversible cross-linking was performed prior to cell lysis (38). Briefly, dithiobis(succinimidyl propionate) (DSP) and dithiobismaleimidoethane (DTME) were used as reversible cross-linkers and were chosen based on their ability to cross-link lysine and cysteine residues, respectively (Fisher Scientific). Cells were treated with increasing doses of either DSP or DTME (0.1, 0.5 and 1 mM) for 30 min. Cell layers were then washed 2× in PBS and treated with Stop solution (Tris–HCl + L-cysteine) for 10 min on ice. Cell layers were washed 1× in PBS, scraped in RIPA buffer, placed in 1.5 ml tubes and passed through a 23-gauge needle to shear DNA. Cell lysates were then centrifuged at 13 000 rpm for 30 min at 4°C. Supernatants were run under both non-reducing and reducing conditions and immunoblotted with V5 antibody (Invitrogen/Life Technologies no. R960-25, 1:5000) followed by secondary antibody (goat anti-mouse HRP 1:5000, PerkinElmer no. NEF822) to determine the optimum dose for each cross-linker and confirm that cross-linking could be reversed via dithiothreitol (DTT) treatment. For proteomic analysis, cells were treated simultaneously with 0.5 mM DSP and 0.1 mM DTME as described above.

Concentrated media and cross-linked cell lysates were immunoprecipitated with V5 antibody (Invitrogen/Life Technologies no. R960-25, 1:250). Cell lysates were treated with DTT to remove the reversible cross-links. Immunoprecipitated samples were run 5–10 mm onto a polyacrylamide gel, stained with Coomassie and partially destained to reveal a single large protein band. Entire gel bands were excised and submitted to the Proteomics Core at UTSW for analysis.

Protein purification

Full-length mouse fibulin-4 including the 5′ UTR was cloned by PCR and ligated into a pcDNA5/FRT/V5-His-TOPO vector (Invitrogen). The fibulin4-V5 vector was co-transfected with a second vector containing Flp recombinase (pOG44, Invitrogen) into Flp-In™-CHO cells as previously described (14). Cells overexpressing fibulin-4-V5 were selected using hygromycin and conditioned media were harvested. Proteins were precipitated using ammonium sulfate and were dialyzed against PBS. The sample was run through a Nickel column (GE Healthcare) and fractions containing fibulin-4 were then passed through a column containing Q-sepharose (GE Healthcare). Q-column fractions containing fibulin-4 were then passed through a Cobalt column and desalted (PD10 columns; GE Healthcare). The resulting protein was >95% pure based on silver staining. Full-length mouse Pcolce was cloned from mouse liver cDNA into pFLAG-CMV™-3 (Sigma) and stably overexpressed in CHO-K1 cells. Following ammonium sulfate precipitation and dialysis against PBS, NaCl and ethylenediaminetetraacetic acid (EDTA) were added to a final concentration of 400 mM and 10 mM, respectively. Protease inhibitor cocktail (Sigma) was also added to the sample. The sample was applied to a 0.6 ml FLAG column (Sigma), washed with buffer containing 50 mM HEPES, 150 mM NaCl, and 0.01% brijL23, and eluted with 0.1 M glycine-saline 0.01% BrijL23 (pH3.0). Tris–HCl (pH.8.0) was added to adjust the sample pH. To eliminate FLAG antibody contamination, elutants were added to the solution with a final concentration of 100 µg/ml 3xFLAG peptide, 0.05% TX-100 and 0.01% brijL23, and then applied to a Protein G column (0.5 ml; GE Healthcare). Samples were eluted from the column with buffer containing 50 mM Tris–HCl (pH7.5), 250 mM NaCl, 0.05% TX-100 and 0.01% brijL23. Sample purity was assessed via immunoblotting and silver stain.

Solid-phase binding assays

Solid-phase binding assays were carried out as described previously (14,63). Briefly, proteins (10 µg/ml) were coated in 96-well plates (Nunc) at 10 µg/ml at 4°C overnight. Plates were blocked in TBS-T containing 5% non-fat dry milk at 4°C overnight. Soluble ligands were added to the plates and incubated for 3 h at room temperature, washed 5× in TBS-T containing 0.025% tween-20 and 2 mM $CaCl_2$. Plates were incubated with primary V5 antibody for 1.5 h (1:5000; Invitrogen no. R960–25), washed and incubated with anti-mouse HRP (1:2500; Bio-Rad no. 170-6516) for 1 h at room temperature. TMB substrate (R&D Systems no. DY999) was incubated for 20 min, and the reaction was stopped with

2 N H_2SO_4. Plates were read at 450 nm using an Optima Fluostar plate reader (BMG Labtech). Data were analyzed using Graphpad Prism software.

Tissue protein extraction and immunoblotting

Ascending aortas were harvested and snap frozen. Tissue protein was extracted using RIPA buffer with protease and phosphatase inhibitors added (Sigma), homogenized in RIPA buffer using a Bullet blender (NextAdvance, Inc.) and centrifuged to clarify lysates. Equal amounts of protein were loaded onto agarose gels, transferred to polyvinylidene difluoride membrane, blocked for 1 h in 5% milk in TBS-T and incubated with primary antibody followed by either rabbit or mouse secondary antibody at a 1:2000 dilution (PerkinElmer, NEF812 and NEF822, respectively). The following primary antibodies were used: LOX-pp (1:1000; kindly provided by P. Trackman; Ref. 60), Pcolce (1:200; Sigma no. C2122) and Gapdh (1:1000, Cell Signal no. 2118L). Immunoblots were quantified using ImageJ software, and data were analyzed using Graphpad Prism software.

MEF isolation and culture, and LOX activity assays

MEFs were isolated from *Efemp2* WT and KO embryos at E12.5–E14.5. The head and internal organs were removed, and the remaining tissue was homogenized using a syringe and 18-gauge needle. Explants were grown in DMEM containing 10% FBS and Pen/Strep (Invitrogen). All experiments were performed on MEFs at Passage 2 or 3. LOX activity assays were performed as described by Trackman PC *et al.* (64). Briefly, equal numbers of WT and KO MEFs were plated in 10 cm dishes. At 70–80% confluency, MEFs were placed in serum-free, phenol red-free DMEM overnight (16 h). Conditioned media were collected and concentrated 40× using a 10000MWCO centrifugal filter (Vivaspin). ECM was extracted in buffer containing 4 M Urea and 0.05 M borate. Following brief sonication, lysates were clarified via centrifugation and concentrated using 3000MWCO centrifugal filters (Millipore). Samples were added to wells of a 96-well plate and were treated ±βAPN in quadruplicate. Samples were then incubated for 15 min at 37°C in buffer with a final concentration of 1.2 M Urea, 0.05 M borate (sodium tetraborate decahydrate, Sigma), 10 μM OxiRed fluorescent probe (10-acetyl-3,7-dihydroxyphenoxazine; BioVision no. 1572-5), 10 mM diaminopentane (Fisher no. 08730) and 2 U/ml HRP. Loxl2 (lysyl oxidase-like protein 2) protein was used as a positive control (R&D Systems no. 2639-AO-010). Plates were read at 544/590 nm using an Optima Fluostar plate reader (BMG Labtech). LOX activity was calculated by subtracting the amount of signal from βAPN-treated samples from untreated samples. Experiments were repeated at least three independent times. Purified Loxl2 protein (R&D Systems no. 2639-AO-010) treated ±βAPN was used as a positive and negative control. Data were graphed and analyzed using GraphPad Prism software, with $P < 0.05$ considered statistically significant.

Pcolce-enhancing activity assays

Assays were performed as described elsewhere (39). Briefly, short procollagen I(α1) containing intact N- and C-terminal propeptides (R&D Systems, no. 6220-CL-020) was incubated at a concentration of 148 nM with recombinant human BMP1 (11.9 nM) and Pcolce (54 nM) in the presence or absence of fibulin-4 (40 nM). BMP1 and Pcolce were also purchased from R&D Systems (no. 1927-ZN-010 and no. 2239-PE-020, respectively). Heparin (50 μg/ml) was used as a positive control. Short type I or type III collagen (R&D Systems, no. 6220-CL-020 and no. 7294-CL-020, respectively) and Pcolce (± fibulin-4, ±heparin) were pre-incubated for 1 h at 37°C. BMP1 was added, and the incubation was continued for an additional 45 min at 37°C. Samples were denatured and separated by sodium dodecyl sulphate–polyacrylamide gel electrophoresis, and proteins were visualized and quantified by silver staining. Assays were performed at least three independent times, and data were analyzed using one-way ANOVA.

Supplementary Material

Supplementary material is available at *HMG* online.

Acknowledgements

We thank the late Jianbin Huang, who generated the SMKO mouse strain and made initial observations, Shelby Chapman for generating the fibulin-4-V5 plasmid and fibulin-4-V5 cells and Jose Cabrera for assistance with graphics and illustrations. We thank Philip Trackman for providing LOX-pp antibody and protocols/troubleshooting for the LOX activity assays and Amy Bradshaw for advice on procollagen processing. We also thank Kate Luby-Phelps and the Live Cell Imaging Core Facility for assistance with SHG/TPEF imaging, John Shelton and the UTSW Pathology Core Lab for paraffin tissue processing and embedding, the Protein Chemistry Technology Core Facility at UTSW, Robert Gerard and the Vector Core at UTSW for assistance with adenovirus production and titering, and the Facility for Electron Microscopy Research (FEMR) at McGill University.

Conflict of Interest statement. None declared.

Funding

This work was supported by The National Institutes of Health (R01HL106305-01 to H.Y. and E.C.D., HD064824 to H.Y., 5T32HL007360-34 to C.L.P., F32HL122076-01 to C.L.P. and NIH S10 RR029731-01 to K.P. (Live Cell Imaging Core Facility at UTSW)), American Heart Association (12EIA8190000 to H.Y.) and the Natural Sciences and Engineering Council of Canada (NSERC RGPIN 355710 to E.C.D.).

References

1. Dasouki, M., Markova, D., Garola, R., Sasaki, T., Charbonneau, N.L., Sakai, L.Y. and Chu, M.L. (2007) Compound heterozygous mutations in fibulin-4 causing neonatal lethal pulmonary artery occlusion, aortic aneurysm, arachnodactyly, and mild cutis laxa. *Am. J. Med. Genet. A*, **143A**, 2635–2641.
2. Erickson, L.K., Opitz, J.M. and Zhou, H. (2012) Lethal osteogenesis imperfecta-like condition with cutis laxa and arterial tortuosity in MZ twins due to a homozygous fibulin-4 mutation. *Pediatr. Dev. Pathol.*, **15**, 137–141.
3. Renard, M., Holm, T., Veith, R., Callewaert, B.L., Ades, L.C., Baspinar, O., Pickart, A., Dasouki, M., Hoyer, J., Rauch, A. *et al.* (2010) Altered TGFbeta signaling and cardiovascular manifestations in patients with autosomal recessive cutis laxa type I caused by fibulin-4 deficiency. *Eur. J. Hum. Genet.*, **18**, 895–901.
4. Hucthagowder, V., Sausgruber, N., Kim, K.H., Angle, B., Marmorstein, L.Y. and Urban, Z. (2006) Fibulin-4: a novel gene for an autosomal recessive cutis laxa syndrome. *Am. J. Hum. Genet.*, **78**, 1075–1080.
5. Giltay, R., Timpl, R. and Kostka, G. (1999) Sequence, recombinant expression and tissue localization of two novel

extracellular matrix proteins, fibulin-3 and fibulin-4. *Matrix Biol.*, **18**, 469–480.
6. Choudhury, R., McGovern, A., Ridley, C., Cain, S.A., Baldwin, A., Wang, M.C., Guo, C., Mironov, A. Jr., Drymoussi, Z., Trump, D. *et al.* (2009) Differential regulation of elastic fiber formation by fibulin-4 and -5. *J. Biol. Chem.*, **284**, 24553–24567.
7. Horiguchi, M., Inoue, T., Ohbayashi, T., Hirai, M., Noda, K., Marmorstein, L.Y., Yabe, D., Takagi, K., Akama, T.O., Kita, T. *et al.* (2009) Fibulin-4 conducts proper elastogenesis via interaction with cross-linking enzyme lysyl oxidase. *Proc. Natl. Acad. Sci. USA*, **106**, 19029–19034.
8. McLaughlin, P.J., Chen, Q., Horiguchi, M., Starcher, B.C., Stanton, J.B., Broekelmann, T.J., Marmorstein, A.D., McKay, B., Mecham, R., Nakamura, T. *et al.* (2006) Targeted disruption of fibulin-4 abolishes elastogenesis and causes perinatal lethality in mice. *Mol. Cell. Biol.*, **26**, 1700–1709.
9. Huang, J., Davis, E.C., Chapman, S.L., Budatha, M., Marmorstein, L.Y., Word, R.A. and Yanagisawa, H. (2010) Fibulin-4 deficiency results in ascending aortic aneurysms: a potential link between abnormal smooth muscle cell phenotype and aneurysm progression. *Circ. Res.*, **106**, 583–592.
10. Hanada, K., Vermeij, M., Garinis, G.A., de Waard, M.C., Kunen, M.G., Myers, L., Maas, A., Duncker, D.J., Meijers, C., Dietz, H.C. *et al.* (2007) Perturbations of vascular homeostasis and aortic valve abnormalities in fibulin-4 deficient mice. *Circ. Res.*, **100**, 738–746.
11. Hoyer, J., Kraus, C., Hammersen, G., Geppert, J.P. and Rauch, A. (2009) Lethal cutis laxa with contractural arachnodactyly, overgrowth and soft tissue bleeding due to a novel homozygous fibulin-4 gene mutation. *Clin. Genet.*, **76**, 276–281.
12. Sawyer, S.L., Dicke, F., Kirton, A., Rajapkse, T., Rebeyka, I.M., McInnes, B., Parboosingh, J.S. and Bernier, F.P. (2013) Longer term survival of a child with autosomal recessive cutis laxa due to a mutation in FBLN4. *Am. J. Med. Genet. A*, **161A**, 1148–1153.
13. Yanagisawa, H. and Davis, E.C. (2010) Unraveling the mechanism of elastic fiber assembly: the roles of short fibulins. *Int. J. Biochem. Cell Biol.*, **42**, 1084–1093.
14. Yanagisawa, H., Davis, E.C., Starcher, B.C., Ouchi, T., Yanagisawa, M., Richardson, J.A. and Olson, E.N. (2002) Fibulin-5 is an elastin-binding protein essential for elastic fibre development in vivo. *Nature*, **415**, 168–171.
15. Nakamura, T., Lozano, P.R., Ikeda, Y., Iwanaga, Y., Hinek, A., Minamisawa, S., Cheng, C.F., Kobuke, K., Dalton, N., Takada, Y. *et al.* (2002) Fibulin-5/DANCE is essential for elastogenesis in vivo. *Nature*, **415**, 171–175.
16. Kobayashi, N., Kostka, G., Garbe, J.H., Keene, D.R., Bachinger, H.P., Hanisch, F.G., Markova, D., Tsuda, T., Timpl, R., Chu, M.L. *et al.* (2007) A comparative analysis of the fibulin protein family. Biochemical characterization, binding interactions, and tissue localization. *J. Biol. Chem.*, **282**, 11805–11816.
17. Maki, J.M., Sormunen, R., Lippo, S., Kaarteenaho-Wiik, R., Soininen, R. and Myllyharju, J. (2005) Lysyl oxidase is essential for normal development and function of the respiratory system and for the integrity of elastic and collagen fibers in various tissues. *Am. J. Pathol.*, **167**, 927–936.
18. Canty, E.G. and Kadler, K.E. (2005) Procollagen trafficking, processing and fibrillogenesis. *J. Cell Sci.*, **118**, 1341–1353.
19. Banos, C.C., Thomas, A.H. and Kuo, C.K. (2008) Collagen fibrillogenesis in tendon development: current models and regulation of fibril assembly. *Birth Defects Res. C. Embryo Today*, **84**, 228–244.
20. Kadler, K.E., Hill, A. and Canty-Laird, E.G. (2008) Collagen fibrillogenesis: fibronectin, integrins, and minor collagens as organizers and nucleators. *Curr. Opin. Cell Biol.*, **20**, 495–501.
21. Yamauchi, M. and Sricholpech, M. (2012) Lysine post-translational modifications of collagen. *Essays Biochem.*, **52**, 113–133.
22. Ishikawa, Y., Vranka, J., Wirz, J., Nagata, K. and Bachinger, H.P. (2008) The rough endoplasmic reticulum-resident FK506-binding protein FKBP65 is a molecular chaperone that interacts with collagens. *J. Biol. Chem.*, **283**, 31584–31590.
23. Hormuzdi, S.G., Penttinen, R., Jaenisch, R. and Bornstein, P. (1998) A gene-targeting approach identifies a function for the first intron in expression of the alpha1(I) collagen gene. *Mol. Cell. Biol.*, **18**, 3368–3375.
24. Rahkonen, O., Su, M., Hakovirta, H., Koskivirta, I., Hormuzdi, S.G., Vuorio, E., Bornstein, P. and Penttinen, R. (2004) Mice with a deletion in the first intron of the Col1a1 gene develop age-dependent aortic dissection and rupture. *Circ. Res.*, **94**, 83–90.
25. Marjamaa, J., Tulamo, R., Abo-Ramadan, U., Hakovirta, H., Frosen, J., Rahkonen, O., Niemela, M., Bornstein, P., Penttinen, R. and Kangasniemi, M. (2006) Mice with a deletion in the first intron of the Col1a1 gene develop dissection and rupture of aorta in the absence of aneurysms: high-resolution magnetic resonance imaging, at 4.7 T, of the aorta and cerebral arteries. *Magn. Reson. Med.*, **55**, 592–597.
26. Smith, L.B., Hadoke, P.W., Dyer, E., Denvir, M.A., Brownstein, D., Miller, E., Nelson, N., Wells, S., Cheeseman, M. and Greenfield, A. (2011) Haploinsufficiency of the murine Col3a1 locus causes aortic dissection: a novel model of the vascular type of Ehlers-Danlos syndrome. *Cardiovasc. Res.*, **90**, 182–190.
27. Le, V.P., Yamashiro, Y., Yanagisawa, H. and Wagenseil, J.E. (2014) Measuring, reversing, and modeling the mechanical changes due to the absence of fibulin-4 in mouse arteries. *Biomech. Model Mechanobiol.*, **13**, 1081–1095.
28. Wenstrup, R.J., Florer, J.B., Brunskill, E.W., Bell, S.M., Chervoneva, I. and Birk, D.E. (2004) Type V collagen controls the initiation of collagen fibril assembly. *J. Biol. Chem.*, **279**, 53331–53337.
29. Wenstrup, R.J., Florer, J.B., Cole, W.G., Willing, M.C. and Birk, D.E. (2004) Reduced type I collagen utilization: a pathogenic mechanism in COL5A1 haplo-insufficient Ehlers-Danlos syndrome. *J. Cell. Biochem.*, **92**, 113–124.
30. Wenstrup, R.J., Florer, J.B., Davidson, J.M., Phillips, C.L., Pfeiffer, B.J., Menezes, D.W., Chervoneva, I. and Birk, D.E. (2006) Murine model of the Ehlers-Danlos syndrome. col5a1 haploinsufficiency disrupts collagen fibril assembly at multiple stages. *J. Biol. Chem.*, **281**, 12888–12895.
31. Campagnola, P.J. and Loew, L.M. (2003) Second-harmonic imaging microscopy for visualizing biomolecular arrays in cells, tissues and organisms. *Nat. Biotechnol.*, **21**, 1356–1360.
32. Chen, X., Nadiarynkh, O., Plotnikov, S. and Campagnola, P.J. (2012) Second harmonic generation microscopy for quantitative analysis of collagen fibrillar structure. *Nat. Protoc.*, **7**, 654–669.
33. Ju, X., Ijaz, T., Sun, H., Lejeune, W., Vargas, G., Shilagard, T., Recinos, A. 3rd, Milewicz, D.M., Brasier, A.R. and Tilton, R.G. (2014) IL-6 regulates extracellular matrix remodeling associated with aortic dilation in a fibrillin-1 hypomorphic mgR/mgR mouse model of severe Marfan syndrome. *J. Am. Heart Assoc.*, **3**, e000476.
34. Hornstra, I.K., Birge, S., Starcher, B., Bailey, A.J., Mecham, R.P. and Shapiro, S.D. (2003) Lysyl oxidase is required for vascular and diaphragmatic development in mice. *J. Biol. Chem.*, **278**, 14387–14393.
35. Velling, T., Risteli, J., Wennerberg, K., Mosher, D.F. and Johansson, S. (2002) Polymerization of type I and III collagens

is dependent on fibronectin and enhanced by integrins alpha 11beta 1 and alpha 2beta 1. *J. Biol. Chem.*, **277**, 37377–37381.
36. Sabatier, L., Chen, D., Fagotto-Kaufmann, C., Hubmacher, D., McKee, M.D., Annis, D.S., Mosher, D.F. and Reinhardt, D.P. (2009) Fibrillin assembly requires fibronectin. *Mol. Biol. Cell*, **20**, 846–858.
37. Maki, J.M., Rasanen, J., Tikkanen, H., Sormunen, R., Makikallio, K., Kivirikko, K.I. and Soininen, R. (2002) Inactivation of the lysyl oxidase gene Lox leads to aortic aneurysms, cardiovascular dysfunction, and perinatal death in mice. *Circulation*, **106**, 2503–2509.
38. Smith, A.L., Friedman, D.B., Yu, H., Carnahan, R.H. and Reynolds, A.B. (2011) ReCLIP (reversible cross-link immuno-precipitation): an efficient method for interrogation of labile protein complexes. *PLoS ONE*, **6**, e16206.
39. Bekhouche, M., Kronenberg, D., Vadon-Le Goff, S., Bijakowski, C., Lim, N.H., Font, B., Kessler, E., Colige, A., Nagase, H., Murphy, G. *et al*. (2010) Role of the netrin-like domain of procollagen C-proteinase enhancer-1 in the control of metalloproteinase activity. *J. Biol. Chem.*, **285**, 15950–15959.
40. Weiss, T., Ricard-Blum, S., Moschcovich, L., Wineman, E., Mesilaty, S. and Kessler, E. (2010) Binding of procollagen C-proteinase enhancer-1 (PCPE-1) to heparin/heparan sulfate: properties and role in PCPE-1 interaction with cells. *J. Biol. Chem.*, **285**, 33867–33874.
41. Djokic, J., Fagotto-Kaufmann, C., Bartels, R., Nelea, V. and Reinhardt, D.P. (2013) Fibulin-3, -4, and -5 are highly susceptible to proteolysis, interact with cells and heparin, and form multimers. *J. Biol. Chem.*, **288**, 22821–22835.
42. Danielson, K.G., Baribault, H., Holmes, D.F., Graham, H., Kadler, K.E. and Iozzo, R.V. (1997) Targeted disruption of decorin leads to abnormal collagen fibril morphology and skin fragility. *J. Cell Biol.*, **136**, 729–743.
43. Chakravarti, S., Magnuson, T., Lass, J.H., Jepsen, K.J., LaMantia, C. and Carroll, H. (1998) Lumican regulates collagen fibril assembly: skin fragility and corneal opacity in the absence of lumican. *J. Cell Biol.*, **141**, 1277–1286.
44. Svensson, L., Aszodi, A., Reinholt, F.P., Fassler, R., Heinegard, D. and Oldberg, A. (1999) Fibromodulin-null mice have abnormal collagen fibrils, tissue organization, and altered lumican deposition in tendon. *J. Biol. Chem.*, **274**, 9636–9647.
45. Hausser, I. and Anton-Lamprecht, I. (1994) Differential ultrastructural aberrations of collagen fibrils in Ehlers-Danlos syndrome types I-IV as a means of diagnostics and classification. *Hum. Genet.*, **93**, 394–407.
46. Holmes, D.F., Watson, R.B., Steinmann, B. and Kadler, K.E. (1993) Ehlers-Danlos syndrome type VIIB. Morphology of type I collagen fibrils formed in vivo and in vitro is determined by the conformation of the retained N-propeptide. *J. Biol. Chem.*, **268**, 15758–15765.
47. Nicholls, A.C., Osse, G., Schloon, H.G., Lenard, H.G., Deak, S., Myers, J.C., Prockop, D.J., Weigel, W.R., Fryer, P. and Pope, F. M. (1984) The clinical features of homozygous alpha 2(I) collagen deficient osteogenesis imperfecta. *J. Med. Genet.*, **21**, 257–262.
48. Kuivaniemi, H., Tromp, G. and Prockop, D.J. (1991) Mutations in collagen genes: causes of rare and some common diseases in humans. *FASEB J.*, **5**, 2052–2060.
49. Kadler, K.E., Baldock, C., Bella, J. and Boot-Handford, R.P. (2007) Collagens at a glance. *J. Cell Sci.*, **120**, 1955–1958.
50. O'Connell, M.K., Murthy, S., Phan, S., Xu, C., Buchanan, J., Spilker, R., Dalman, R.L., Zarins, C.K., Denk, W. and Taylor, C.A. (2008) The three-dimensional micro- and nanostructure of the aortic medial lamellar unit measured using 3D confocal and electron microscopy imaging. *Matrix Biol.*, **27**, 171–181.
51. Levene, C.I. (1961) Collagen as a tensile component in the developing chick aorta. *Br J Exp. Pathol.*, **42**, 89–94.
52. Kato, H., Suzuki, H., Tajima, S., Ogata, Y., Tominaga, T., Sato, A. and Saruta, T. (1991) Angiotensin II stimulates collagen synthesis in cultured vascular smooth muscle cells. *J Hypertens.*, **9**, 17–22.
53. Amento, E.P., Ehsani, N., Palmer, H. and Libby, P. (1991) Cytokines and growth factors positively and negatively regulate interstitial collagen gene expression in human vascular smooth muscle cells. *Arterioscler. Thromb.*, **11**, 1223–1230.
54. Steiglitz, B.M., Kreider, J.M., Frankenburg, E.P., Pappano, W.N., Hoffman, G.G., Meganck, J.A., Liang, X., Hook, M., Birk, D.E., Goldstein, S.A. *et al*. (2006) Procollagen C proteinase enhancer 1 genes are important determinants of the mechanical properties and geometry of bone and the ultrastructure of connective tissues. *Mol. Cell. Biol.*, **26**, 238–249.
55. Nissen, R., Cardinale, G.J. and Udenfriend, S. (1978) Increased turnover of arterial collagen in hypertensive rats. *Proc. Natl. Acad. Sci. USA*, **75**, 451–453.
56. Wilson, J.S., Baek, S. and Humphrey, J.D. (2013) Parametric study of effects of collagen turnover on the natural history of abdominal aortic aneurysms. *Proc. Math. Phys. Eng. Sci.*, **469**, 20120556.
57. Heegaard, A.M., Corsi, A., Danielsen, C.C., Nielsen, K.L., Jorgensen, H.L., Riminucci, M., Young, M.F. and Bianco, P. (2007) Biglycan deficiency causes spontaneous aortic dissection and rupture in mice. *Circulation*, **115**, 2731–2738.
58. Kalamajski, S., Liu, C., Tillgren, V., Rubin, K., Oldberg, A., Rai, J., Weis, M. and Eyre, D.R. (2014) Increased C-telopeptide cross-linking of tendon type I collagen in fibromodulin-deficient mice. *J. Biol. Chem.*, **289**, 18873–18879.
59. Huang, J., Yamashiro, Y., Papke, C.L., Ikeda, Y., Lin, Y., Patel, M., Inagami, T., Le, V.P., Wagenseil, J.E. and Yanagisawa, H. (2013) Angiotensin-converting enzyme-induced activation of local angiotensin signaling is required for ascending aortic aneurysms in fibulin-4-deficient mice. *Sci. Transl. Med.*, **5**, 183ra158, 181–111.
60. Vora, S.R., Guo, Y., Stephens, D.N., Salih, E., Vu, E.D., Kirsch, K. H., Sonenshein, G.E. and Trackman, P.C. (2010) Characterization of recombinant lysyl oxidase propeptide. *Biochemistry*, **49**, 2962–2972.
61. Yamauchi, M. and Shiiba, M. (2008) Lysine hydroxylation and cross-linking of collagen. *Methods Mol. Biol.*, **446**, 95–108.
62. Davis, E.C. (1993) Smooth muscle cell to elastic lamina connections in developing mouse aorta. Role in aortic medial organization. *Lab. Invest.*, **68**, 89–99.
63. Reinhardt, D.P., Sasaki, T., Dzamba, B.J., Keene, D.R., Chu, M. L., Gohring, W., Timpl, R. and Sakai, L.Y. (1996) Fibrillin-1 and fibulin-2 interact and are colocalized in some tissues. *J. Biol. Chem.*, **271**, 19489–19496.
64. Palamakumbura, A.H. and Trackman, P.C. (2002) A fluorometric assay for detection of lysyl oxidase enzyme activity in biological samples. *Anal. Biochem.*, **300**, 245–251.
65. Tsamis, A., Krawiec, J.T. and Vorp, D.A. (2013) Elastin and collagen fibre microstructure of the human aorta in ageing and disease: a review. *J. R. Soc. Interface*, **10**, 20121004.
66. Nakai, A., Satoh, M., Hirayoshi, K. and Nagata, K. (1992) Involvement of the stress protein HSP47 in procollagen processing in the endoplasmic reticulum. *J. Cell Biol.*, **117**, 903–914.
67. Moschcovich, L., Bernocco, S., Font, B., Rivkin, H., Eichenberger, D., Chejanovsky, N., Hulmes, D.J. and Kessler, E. (2001)

Folding and activity of recombinant human procollagen C-proteinase enhancer. *Eur. J. Biochem.*, **268**, 2991–2996.
68. Atabai, K., Jame, S., Azhar, N., Kuo, A., Lam, M., McKleroy, W., Dehart, G., Rahman, S., Xia, D.D., Melton, A.C. *et al.* (2009) Mfge8 diminishes the severity of tissue fibrosis in mice by binding and targeting collagen for uptake by macrophages. *J. Clin. Invest.*, **119**, 3713–3722.
69. Siegel, R.C., Pinnell, S.R. and Martin, G.R. (1970) Cross-linking of collagen and elastin. Properties of lysyl oxidase. *Biochemistry*, **9**, 4486–4492.